---

**Proceedings Paper:**
Drummond, R. orcid.org/0000-0002-2586-1718, Valmorbida, G. and Duncan, S.R. (2017) Equivalent Circuits for Electrochemical Supercapacitor Models. In: Dochain, D., Henrion, D. and Peaucelle, D., (eds.) IFAC-PapersOnLine. 20th IFAC World Congress, 09-14 Jul 2017, Toulouse, France. Elsevier BV , pp. 2671-2676.

https://doi.org/10.1016/j.ifacol.2017.08.551

---

# Equivalent Circuits for Electrochemical Supercapacitor Models ⋆

**Ross Drummond** * **Giogio Valmorbida** ** **Stephen R. Duncan** *

* *Dept. of Engineering Science, Universiy of Oxford, Oxford, UK, OX1 3PJ (e-mail: ross.drummond@eng.ox.ac.uk).*
** *Laboratoire des Signaux & Systèmes, CentraleSupélec, CNRS, Univ. Paris-Sud, Université Paris-Saclay, 3 Rue Joliot-Curie, Gif–sur–Yvette, 91192, France (e-mail:giorgio.valmorbida@l2s.centralesupelec.fr)*

Abstract: Circuit and electrochemical models of supercapacitor electrical energy storage devices are related via their energy dissipation. A method for the synthesis of linear, low-order finite dimensional circuits from nonlinear infinite dimensional electrochemical partial differential equations is analysed with this method involving discretisation, linearisation, model order reduction and circuit synthesis. It is shown that a circuit with three time constants sufficiently captures the input/output response of the electrochemical model. Using absolute stability, the local nature of the resistance of the nonlinear electrochemical model is shown. The problem of supercapacitor design is also discussed, with the device capacitance and resistance being linked to its electrochemical parameters.

*Keywords:* Supercapacitors, modelling, absolute stability theory.

## INTRODUCTION

This paper uses control theory to relate two modelling approaches for electrochemical energy storage devices known as supercapacitors. One of these approaches uses a set of partial differential equations derived from the electrochemistry, while the other is based on equivalent circuits. Supercapacitors, summarised in Burke (2000), are energy storage devices that store electrical energy electrostatically on porous electrodes typically made from carbon. Because they store charge electrostatically, supercapacitors have higher power densities, reduced temperature dependence, reduced degradation, but they have lower energy densities compared to lithium ion batteries. The typical construction of a supercapacitor is similar to a battery and is shown in Figure 1 with two porous electrodes separated by an electrically insulating separator. Flowing thorough the device is an aqueous ionic electrolyte carrying charge. Current is transferred to and from the system via current collectors. Supercapacitors have higher energy densities than standard dielectric capacitors composed of flat plates as the distance between the charges in the electrode and the electrolyte is typically the width of a solvated water molecule that surrounds the ions. The interface between the solid electrode and the electrolyte is known as the double layer. Since capacitance is inversely proportional to charge separating distance, this results in high capacitance values. Also, the highly porous nature of the electrodes means they have high surface areas which increases the amount of charge that can be stored. Currently, capacitance values are in the range of several hundreds of farads per gram, although this figure is increasing with the development of new materials such as metal organic frameworks of Sheberla et al. (2016). For more details on supercapacitors and their charge storing mechanism, see Lu et al. (2013).

The majority of supercapacitor research has focussed on the development of new materials to increase capacitance. Recently, control theory has been employed to understand how the supercapacitor stores and dissipates energy during its operation leading to improvements in design and implementation. This approach requires a suitable model of the device with there being two main modelling approaches. The first uses (generally nonlinear) partial differential equations (PDEs) to describe the electrochemistry and the second maps the current to voltage using a circuit composed of resistors and capacitors. The PDE electrochemical models describe the evolution of the potential gradients and the ionic concentration in the spatially homogenised porous electrodes using conservation relations. These models are relatively high fidelity, which makes them particularly useful for supercapacitors designers, as numerical experiments can then be used to reduce the number of time consuming physical experiments. By contrast, circuit models are generally linear and have a state-space that is finite-dimensional and low order. They are typically used in implementation due to their low computational complexity as in Dey et al. (2016). They are also used to obtain models from electro-impedance spectroscopy data as in Rafik et al. (2007). Examples of electrochemical models include Allu et al. (2014); Verbrugge and Liu (2005); Srinivasan and Weidner (1999); Romero-Becerril and Alvarez-Icaza (2010); Drummond et al. (2015); d'Entremont and Pilon (2014). Equivalent circuit models include Robinson (2010); Buller et al. (2001); Rafik et al. (2007) and are reviewed in Zhang et al. (2015).

⋆ This work was supported in part by funding from the EPSRC.

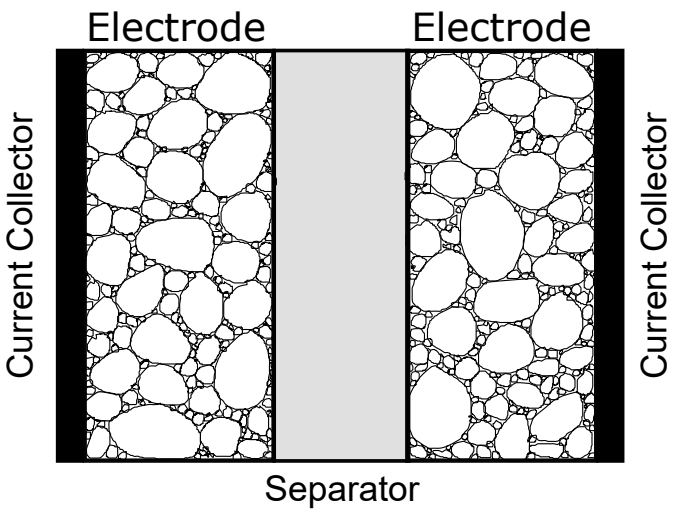


Figure 1. Typical construction of a supercapacitor.

| | Definition | Value | Units |
|---|---|---|---|
| Global Parameters | | | |
| $T$ | Temperature | 298 | K |
| $t_+$ | Transference number | 0.75 | |
| $\frac{dq_{+/-}}{dq}$ | Charge transfer coef. | -0.5 | |
| $c_0$ | Rest ionic concentration. | 500 | mol m$^{-3}$ |
| Electrode Parameters | | | |
| $\kappa$ | Electrolyte conductivity | 0.026 | S m$^{-1}$ |
| $D$ | Diffusion coef. | $3.67 \times 10^{-11}$ | m$^2$ s$^{-1}$ |
| $\epsilon$ | Porosity factor | 0.67 | |
| $\sigma$ | Electrode conductivity | $1.14 \times 10^{-4}$ | S m$^{-1}$ |
| $aC$ | Specific capacitance | $1.87 \times 10^{5}$ | F m$^{-2}$ |
| $L_{elec}$ | Electrode length | $25 \times 10^{-6}$ | m |
| Separator Parameters | | | |
| $\kappa$ | Electrolyte conductivity | $5.78 \times 10^{-5}$ | S m$^{-1}$ |
| $D$ | Diffusion coef. | $8.19 \times 10^{-15}$ | m$^2$ s$^{-1}$ |
| $\epsilon$ | Porosity factor | 0.6 | |
| $L_{sep}$ | Separator length | $10 \times 10^{-6}$ | m |

Table 1. Parameters of the electrochemical supercapacitor model obtained from Drummond et al. (2016a).

The aim of this paper is to study the two modelling approaches by considering how they dissipate energy. This paper will extend the authors' previous results of Drummond et al. (2017), Drummond et al. (2016b) and Valmorbida et al. (2016). A procedure for synthesizing circuits from an electrochemical supercapacitor model was introduced in Drummond et al. (2017) and this paper will analyse how the steps of this synthesis affect the resulting current to voltage dynamics. The dynamics of the synthesized circuits are compared to the dynamics of an electrochemical model whose current to voltage gain is upper bounded using absolute stability theory given in Drummond et al. (2016b). In this paper, we show how the gain of this system changes with the local domain of the state-space and how this affects the accuracy of the equivalent circuits models.

Electrochemical interpretations of circuits have already been proposed in the literature, but these interpretations are typically not derived from the electrochemical PDE equations in a methodical manner. The problem of designing supercapacitors was considered in Robinson (2010) with the circuit representing the pore dynamics. A set of supercapacitor circuits including the Cauer and Foster forms of the first kind was described in Zhang et al. (2015). A phenomenological circuit for lithium ion batteries was proposed in von Srbik et al. (2016) that used spatial discretisation to synthesize a circuit with nonlinear elements. The synthesis method here is general as it enables a wide class of circuits with different topologies to be synthesized from a set of electrochemical equations, with the synthesis procedure being both methodical and computationally efficient. In this setting, the circuits are considered to be state-space realisations of the impedance function with the non-uniqueness of the realisations resulting in many circuits being realisable.

Due to space constraints, proofs are omitted for the stability conditions in the propositions although these proofs can be easily seen from those of the circle and Popov criterions of absolute stability and the $\mathcal{L}_2$ gain bounds of linear systems from Boyd et al. (1994).

*Outline*

The paper is structured as follows. The electrochemical model equations are described in Section 1. The circuit synthesis method is presented and analysed in terms of its resistance in Section 2. The local $\mathcal{L}_2$ gain of the nonlinear electrochemical model is analysed in Section 3 and the application to supercapacitor design is considered.

*Notation*

The set of real valued matrices of dimension $n$ are denoted $\mathbb{R}^n$, the set of positive definite symmetric matrices of dimension $n$ are $\mathbb{S}^n_{>0}$ and the set of diagonal positive and positive semidefinite matrices of dimension $n$ are respectively $\mathbb{D}^n_{>0}$ and $\mathbb{D}^n_{\geq 0}$. The row vector of dimension $n$ containing 1's is denoted $\mathbf{1}^n$. The $j^{th}$ row of a vector is denoted by the subscript $j$. The sublevel sets of a function $V(x)$ are denoted $\mathcal{E}(V,\alpha) = \{x \in \mathbb{R}^n | V(x) \leq \alpha\}$.

## 1. ELECTROCHEMICAL SUPERCAPACITOR MODEL

The supercapacitor electrochemical model used to synthesize the equivalent circuits is now described. The partial differential algebraic equations describing the electrochemistry were obtained from Verbrugge and Liu (2005). In the electrode, the dynamics are

$$\epsilon \frac{\partial c}{\partial t} = D\frac{\partial^2 c}{\partial x^2} - K_1 \frac{\partial(\phi_1 - \phi_2)}{\partial t}, \tag{1a}$$

$$aC\frac{\partial(\phi_1 - \phi_2)}{\partial t} = \sigma \frac{\partial^2 \phi_1}{\partial x^2}, \tag{1b}$$

$$K_2 \frac{\partial}{\partial x}\ln(c) + \sigma\frac{\partial \phi_1}{\partial x} + \kappa \frac{\partial \phi_2}{\partial x}, + i = 0 \tag{1c}$$

where

$$K_1 = \frac{aC}{F}\left(t_- \frac{dq_+}{dq} + t_+ \frac{dq_-}{dq}\right), \; K_2 \; = \frac{\kappa\, RT}{F}(t_+ - t_-), \tag{2}$$

with the model parameters given in Table 1. The model states are ionic concentration $c$, electro-potential in the

electrode $\phi_1$ and the electro-potential in the electrolyte $\phi_2$. The model output is the voltage $v$ and the input is the current density $i$. The diffusion of the electrolyte ions, with a forcing term due to the potential gradient across the double layer, is described by (1a). The relaxation of the potential difference across the double layer is described by (1b). Conservation of current is enforced by (1c), which can be considered as an infinite dimensional form of Kirchoff's current law. The model equations in the separator are the same as (1) except without any terms involving $\phi_1$ or $\phi_1 - \phi_2$ because the separator is an electrical insulator. These dynamics can be considered as coupled diffusion equations with forcing terms whose solutions are pinned to the manifold (1c) with the input entering via the manifold. The boundary conditions between the current collector and the electrode are

$$\begin{aligned} \frac{\partial \phi_1}{\partial x} &= -\frac{i}{\sigma}, & \phi_1|_{x=0} &= 0, \\ \frac{\partial \phi_2}{\partial x} &= 0, & \frac{\partial c}{\partial x} &= 0, \end{aligned} \tag{3}$$

and those at the electrode/separator boundary are

$$\begin{aligned} &\frac{\partial \phi_1}{\partial x} = 0, \quad D\frac{\partial c}{\partial x}\bigg|_{elec} = D\frac{\partial c}{\partial x}\bigg|_{sep} \\ &K_2\frac{\partial \ln(c)}{\partial x} + \kappa\frac{\partial \phi_2}{\partial x}\bigg|_{elec} = K_2\frac{\partial \ln(c)}{\partial x} + \kappa\frac{\partial \phi_2}{\partial x}\bigg|_{sep}. \end{aligned} \tag{4}$$

The subscripts *sep* and *elec* respectively describe the separator and electrode domains. These are a combination of Neumann and Dirichlet conditions. The Neumann conditions ensure that all the current is in the solid phase at the current collectors and in the liquid phase at the separator, while the Dirichlet condition imposes a reference potential. The model output is the voltage $v = \phi_1|_{x=0} - \phi_1|_{x=L}$ where $L = 2L_{elec} + L_{sep}$ is the total length of the domain.

## 2. EQUIVALENT CIRCUITS

Using the method proposed in Drummond et al. (2017), a set of circuits is generated to locally approximate the nonlinear partial differential equations of (1). This method follows:

[1] Begin with electrochemical PDEs that describe the system in sufficient detail.
[2] Obtain a finite state realisation by discretising the PDEs in space.
[3] Linearise this model around its equilibrium point.
[4] Check positive realness of the resulting impedance function.
[5] Reduce the model order using the balanced truncation method.
[6] Synthesize circuits via expansions of the impedance function.

Step [2] gives a finite dimensional approximation to the infinite dimensional system with this approximation being validated by experimental data in Drummond et al. (2016a). The discretisation method affects how well the finite dimensional approximation captures the PDEs, and in this paper, spectral collocation is used as in Drummond et al. (2015). The linearisation of [3] results in the synthesized circuits having fixed resistors and capacitors. [4] is a necessary condition for the synthesis of a passive

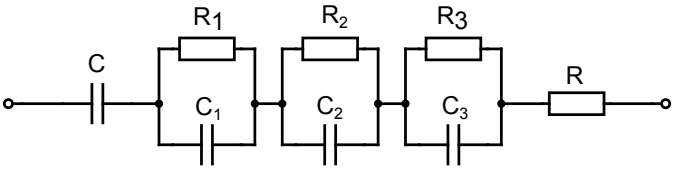


Figure 2. Foster form of the first kind circuit with three *RC* pairs. Image obtained from Drummond et al. (2017).

circuit from an impedance function. [5] allows low order circuits to be realised, as the number of grid points of the PDE discretisation is generally greater than the number of circuit branches. The synthesis of [6] uses standard techniques of circuit theory from Guillemin (1977). In this paper, Foster form of the first kind circuits are realised, although it is stressed that a much wider class of circuit could also be realised using alternative realisations of the impedance function. The choice of model reduction also affects the class of circuits considered. We have chosen the balanced method [Xia et al. (2012)] due to its generality and the fact that it is passivity preserving.

The three branch Foster form realisation equivalent circuit is shown in Figure 2, where the combination $R_jC_j$ is referred to as an *RC* branch. This circuit has dynamics

$$\begin{bmatrix} \dot{x}_{c,i} \\ \dot{x}_{c,d} \end{bmatrix} = \begin{bmatrix} 0 & 0 \\ 0 & -(\mathbf{RC})^{-1} \end{bmatrix} \begin{bmatrix} x_{c,i} \\ x_{c,d} \end{bmatrix} + \begin{bmatrix} \frac{1}{C_c} \\ \mathbf{C}^{-1}\mathbf{1}^{n_{c,d}T} \end{bmatrix} i \tag{5a}$$

$$v_{c,i} = x_{c,i} \tag{5b}$$

$$v_{c,d} = \mathbf{1}^{n_{c,d}} x_{c,d} + R_s i \tag{5c}$$

$$v_c = v_{c,i} + v_{c,d} \tag{5d}$$

where $\mathbf{R} = diag(R_1, \ldots, R_{n_d})$ and $\mathbf{C} = diag(C_1, \ldots, C_{n_d})$ with $R_j$ and $C_j$ being the resistors and capacitor of the $j^{th}$ *RC* branch. The state-space model in (5) is formed of "integrated states" $x_{c,i} \in \mathbb{R}$ and "dissipative states" $x_{c,d} \in \mathbb{R}^{n_{c,d}}$. The integrator states store the energy supplied by the current, while the dissipative states describe the losses. The $\mathcal{L}_2$ gain from current to voltage of the dissipative dynamics of (5) satisfying $\gamma_{circ}\|i\|_2 \geq \|v_{c,d}\|_2$ is used to evaluate how the dynamics are affected by the number of circuit *RC* branches. This gain corresponds to the resistance. Using the Lyapunov function $V_c(x_{c,d}) = x_{c,d}^T P x_{c,d}$, the $\mathcal{L}_2$ gain is upper bounded by solving the semi-definite program (SDP):

*Proposition 1.* If there exists a matrix $P \in \mathbb{S}_{>0}^{n_{c,d}}$ and scalar $\gamma_{circ} > 0$ such that the solution of

$$\text{minimise } \gamma_{circ} \tag{6a}$$

$$\begin{bmatrix} A_{circ}P + PA_{circ}^T + \mathbf{1}^{n_{c,d}T}\mathbf{1}^{n_{c,d}} & PB_{circ} + \mathbf{1}^{n_{c,d}T}R_s \\ B_{circ}^T P + R_s\mathbf{1}^{n_{c,d}} & R_s^2 - \gamma_{circ} \end{bmatrix} < 0 \tag{6b}$$

where $A_{circ} = -(\mathbf{RC})^{-1}$ and $B_{circ} = \mathbf{C}^{-1}\mathbf{1}^{n_{c,d}T}$ is feasible, then $\gamma_{circ}$ is a global minimum upper bound for $\gamma_{circ}\|i\|_2 \leq \|v_{c,d}\|_2$.

Figure 3 shows the variation of the computed $\mathcal{L}_2$ gain bound with number of circuit *RC* branches that are related to the number of time constants in the system. For the circuits synthesized from the electrochemical supercapacitor model defined by the parameters of Table 1, there was little benefit in having a circuit with more than three *RC*

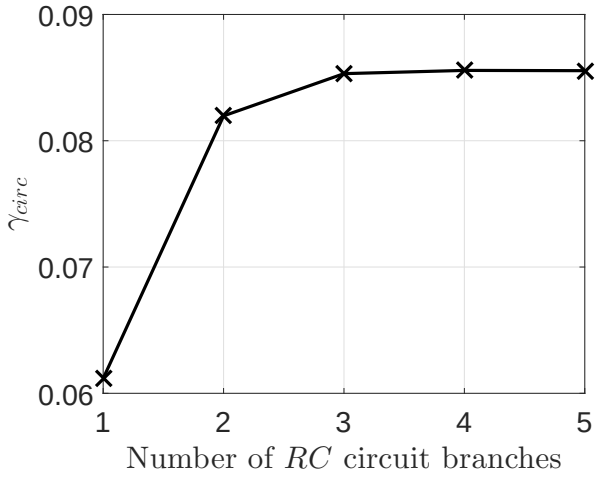


Figure 3. Variation of the $\mathcal{L}_2$ gain bound of the synthesized circuit with the number of $RC$ pairs.

branches as the $\mathcal{L}_2$ gain converged. This gives an electrochemical justification for the popularity of three branch $RC$ circuits in the literature as in Zhang et al. (2015). A hypothesis for the physical reason for the three branch $RC$ circuit is that there are three dynamical equations in the model, (1a) and (1b) in the electrodes and (1a) in the separator without the $\partial(\phi_1 - \phi_2)/\partial t$ term and with different parameters.

## 3. LOCAL $\mathcal{L}_2$ GAIN OF ELECTROCHEMICAL MODEL

In this section, we will preserve the nonlinearity of the electrochemical equations of (1) to analyse its impact on the induced $\mathcal{L}_2$ gain. The circuits developed in Section 2 are derived from the electrochemical equations of (1). In order to understand the $\mathcal{L}_2$ gain of these circuits, the $\mathcal{L}_2$ gain of the underlying electrochemical model has to be considered. The nonlinearity of (1) means that its induced $\mathcal{L}_2$ gain depends upon the magnitude of the input and such a local property may affect the parameters obtained for the linearised circuits. A method of computing this gain for the discretised version of (1) was proposed in Drummond et al. (2016b). This method involves a change in co-ordinates of $c$ such the model describes the evolution of concentration deviations $\tilde{c}$ around an equilibrium $c_0$ with $c = c_0 + \tilde{c}$. This changes $\ln(c)$ in (1c) to $\ln(1 + \tilde{c}/c_0) + \ln(c_0)$. Noting that $\partial/\partial t \ \ln(c_0) = \partial^2/\partial x^2 \ \ln(c_0) = \partial/\partial x \ \ln(c_0) = 0$, the discretised version of the electrochemical model can be represented as

$$\dot{x}_i = B_{int} i \tag{7a}$$
$$v_i = C_{int} x_i \tag{7b}$$

$$\dot{x}_d = A x_d + B_\psi \psi(y) + B_i i \tag{8a}$$
$$v_d = C_d x_d + D_\psi \psi(y) + D_i i \tag{8b}$$
$$y = C_\psi x_d \tag{8c}$$
$$\psi_j(y_j) = \ln(1 + y_j), \quad j = 1, \ldots, m \tag{8d}$$

$$v = v_i + v_d \tag{9}$$

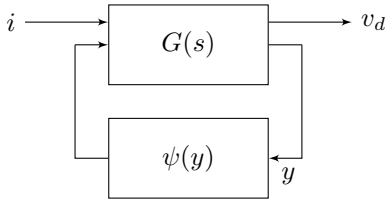


Figure 4. A Lur'e system composed of the feedback interconnection of a linear system with a sector bounded nonlinearity.

which uses a similar notation to (5) with $x_i \in \mathbb{R}$ and $x_d \in \mathbb{R}^{n_d}$ corresponding to stored and dissipated energy. The input and output variables are defined as $v_i \in \mathbb{R}$, $y \in \mathbb{R}^m$, $i \in \mathbb{R}$, $v_d \in \mathbb{R}$. The gain from $\int_0^T i \, dt$ to $v_i$ of the integrator system (7) is $(C_{int}B_{int})^{-1}$ and can be seen to be the capacitance of the device from the definition of charge $Q = \int_0^T i \, dt = Cv_i$. When $y_j \in (-1, \infty)$, the nonlinearity $\ln(1+y_j)$ lies in a (local) sector. Then (8) can be regarded as a Lur'e system [Khalil (2002)]. A Lur'e system is given by the feedback interconnection of a linear system with a nonlinearity which is decentralised

$$\psi(y) = [\psi_1(y_1), \quad \psi_2(y_2), \quad \ldots, \psi_m(y_m)]^T, \tag{10}$$

and sector bounded

$$\frac{\psi_j(y_j)}{y_j} \in \mathbf{\Delta}_j = [\underline{\delta_j}, \overline{\delta_j}] \quad \forall y \in \mathcal{Y}_0 \subseteq \mathcal{Y} \subseteq \mathbb{R}^m. \tag{11}$$

as in Figure 4. Due to the logarithmic nonlinearity of (8d) being undefined for $y_j < -1$ and $\lim_{y_j \to -1} \ln(1 + y_j) = -\infty$, the analysis of (8) was constrained to a local domain $\mathcal{Y}_0$. Define $\mathcal{X}_0 = \{x | y(x) \in \mathcal{Y}_0\}$. The set $\mathcal{Y}_0$, defining the region in the state-space where the nonlinearity is sector bounded, has the form $\mathcal{Y}_0 = \{y : (\overline{y}_j - y_j)(y_j - \underline{y}_j) \geq 0 \text{ for } j = 1, \ldots, m\}$. The bounds $\overline{y}_j$, $\underline{y}_j$ are chosen to contain the reachable set from bounded inputs satisfying $\|i(t)\|_2 \leq \alpha$ with $\alpha \in \mathbb{R}_{>0}$.

To analyse (8), the Lur'e type Lyapunov function is used

$$V(x_d) = x_d^T P x_d + 2 \sum_{j=1}^{m} \lambda_j \int_0^{y_j} \psi_j(v) \, dv \tag{12}$$

where $P \in \mathbb{S}^{n_d}_{>0}$ and $\lambda_j \geq 0$. Since the integral terms in (12) are non-negative, we have

$$\underline{V}(x_d) = x_d^T P x_d \leq V(x_d). \tag{13}$$

Solving the following SDP gives an upper bound for the locally induced $\mathcal{L}_2$ gain related to the resistance

*Proposition 2.* If there exists $\Lambda = diag(\lambda_1, \ldots, \lambda_m) \in \mathbb{D}^m_{\geq 0}$, $P \in \mathbb{S}^{n_d}_{>0}$, $T \in \mathbb{D}^m_{>0}$ and scalar $\gamma > 0$ such that the solution of

$$\text{minimise } \gamma \tag{14a}$$
$$\text{subject to } M_\Delta \leq 0, \ \mathcal{E}(\underline{V}, \alpha) \subseteq \ \mathcal{X}_0 \tag{14b}$$

with $M_\Delta$ as in (15) where $\overline{\Delta} = diag(\overline{\delta}_1, \ldots, \overline{\delta}_m)$ and $\underline{\Delta} = diag(\underline{\delta}_1, \ldots, \underline{\delta}_m)$ is feasible, then $\gamma$ is an upper bound on the locally induced $\mathcal{L}_2$ gain $\gamma$ satisfying $\gamma \|i\|_2 \geq \|v_d\|_2$ for inputs of bounded energy $\|i\|_2 \leq \alpha^{\frac{1}{2}}$.

From (13) we have $\mathcal{E}(\underline{V}, \alpha) \supseteq \mathcal{E}(V, \alpha)$. Thus (14b) implies $\mathcal{E}(V, \alpha) \subseteq \mathcal{Y}_0$. The inclusion condition is formulated as an LMI condition in Boyd et al. (1995).

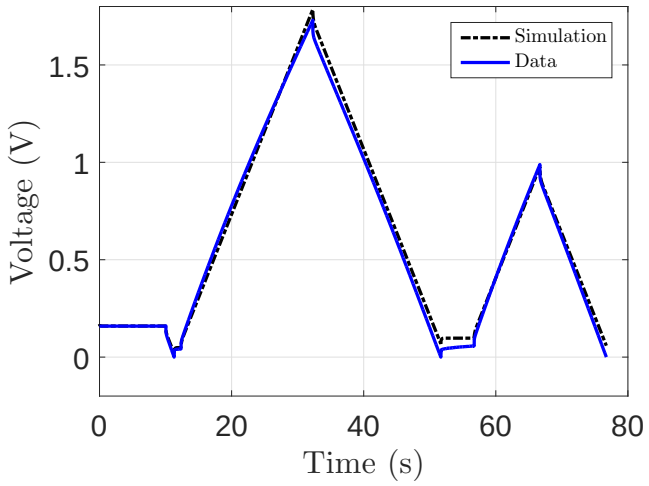


(a) Voltage response.

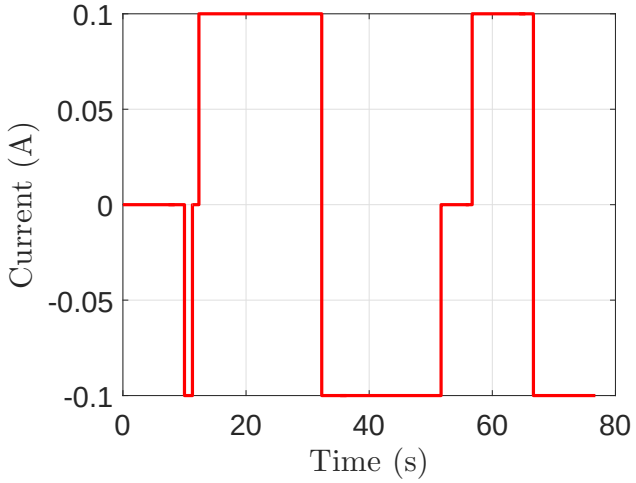


(b) Current profile.

Figure 5. Experimental data and simulation of the discretised version of (1) for a pulsed current charge. Data and figures obtained from Drummond et al. (2016a).

The $\mathcal{L}_2$ bounds of Proposition 2 are evaluated using the supercapacitor described by the parameters of Table 1. Figure 5a shows the voltage response from the pulsed current charge of figure 5b from the simulation of (1) and experimental data obtained from Drummond et al. (2016a). To evaluate the local induced gains, we consider symmetric bounds in $\mathcal{Y}_0$, yielding $\mathcal{Y}_0(\beta) = \{y \in \mathbb{R}^m : \beta^2\overline{y}_j^2 - y_j^2 \geq 0 \text{ for } j = 1, \ldots, m\}$ where $\beta \geq 0$ is a parameter that scales the set and as a consequence, impacts on the sector parameters $\overline{\delta}_j$, $\underline{\delta}_j$.

Figure 6 shows that the solution to (14) for different values of $\alpha$, bounds on the input energy $\|i\|_2 \leq \alpha$, and $\beta$. The figure illustrates that the $\mathcal{L}_2$ gain of the system varies both with the domain $\mathcal{X}_0$ and the input energy. This is in sharp contrast to the linear model where the gain is independent of the magnitude of the input.

A major trade-off in the choice of supercapacitor model is that between complexity and fidelity. One application that warrants the increased detail associated with an electrochemical model is supercapacitor design. The resistance

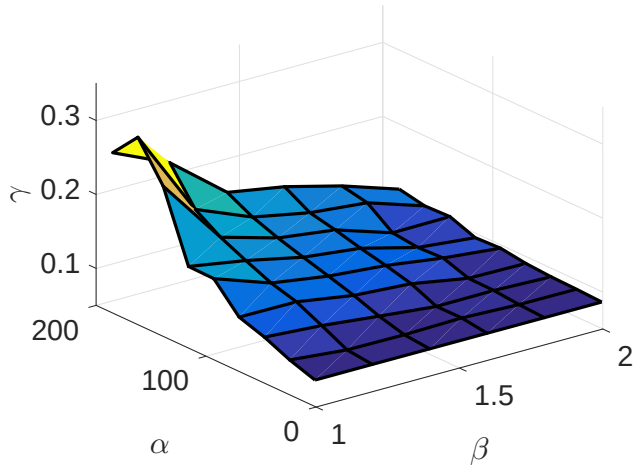


Figure 6. Local $\mathcal{L}_2$ gain of (8). The bounds on $\gamma$ from proposition 2 are computed for different values of the parameter $\beta$ which scales the local domain $\mathcal{Y}_0$.

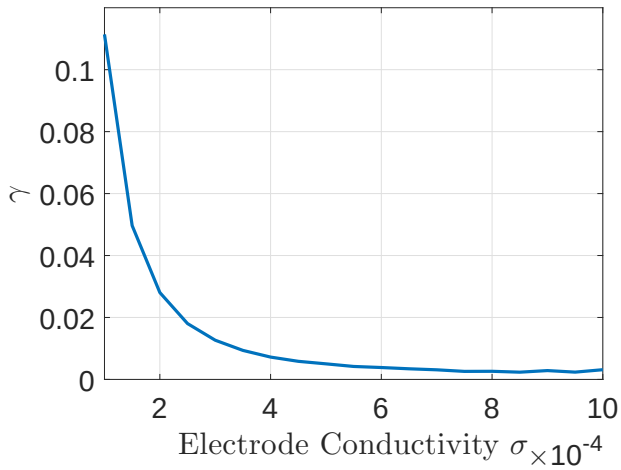


Figure 7. Variation of the bound of the induced $\mathcal{L}_2$ gain $\gamma$ with electrode conductivity $\sigma$.

is a key prperty of the supercapacitor and is desired to be minimised as it characterises losses. Figure 7 shows the variation of resistance, defined by $\gamma$, with the electrode conductivity $\sigma$. The values of $\gamma$ correspond to the solution of (14) with $\beta = 1$ and $\alpha = 0.65$. The inverse relation of Figure 7 relates to the definition of conductivity, and it shows that the PDEs of (1) capture this relationship. The ability to link the performance of a supercapacitor to its electrical parameters will reduce the number of costly and time consuming physical experiments that have to be carried out by designers, replacing them with the solutions of SDPs. In Drummond et al. (2016b), electrochemical performance was linked to the variation of electrode length. The electrochemical model also gives insight into the evolution of the internal state of the supercapacitor during a charge that can flag up regions of ionic depletion for example. These results are not immediately obvious using circuits.

$$M_\Delta = \begin{bmatrix} A^TP + PA + C_d^TC_d - \overline{\Delta}\underline{\Delta} & PB_p + A^TC_\psi^T\Lambda + C_d^TD_\psi + 0.5C_\psi^T(\overline{\Delta} - \underline{\Delta})T & PB_i + C_d^TD_i \\ B_\psi^TP + \Lambda C_\psi A + D_\psi^TC_d + 0.5(\overline{\Delta} - \underline{\Delta})TC_\psi & \Lambda C_\psi B_\psi + B_\psi^TC_\psi^T\Lambda + D_\psi^TD_\psi - T & \Lambda C_\psi B_i + D_\psi^TD_i \\ B_i^TP + D_iC_d & B_i^TC_\psi^T\Lambda + D_iD_\psi & D_iD_i - \gamma \end{bmatrix} \tag{15}$$

## 4. CONCLUSION

This paper considered the energy dissipation properties of nonlinear electrochemical models and linear circuits describing the dynamics of supercapacitors. A synthesis procedure for the circuits is analysed and it is shown that a circuit with three time constants sufficiently captures the input/output response of the linearised electrochemical equations. The local nature of the $\mathcal{L}_2$ gain from current to voltage of the nonlinear electrochemical model was shown using absolute stability theory. This result was related to supercapacitor design, with the electrochemical parameters of the supercapacitor being linked to its electrical properties.

## REFERENCES


Allu, S., Velamur Asokan, B., Shelton, W.A., Philip, B., and Pannala, S. (2014). A generalized multi-dimensional mathematical model for charging and discharging processes in a supercapacitor. *Journal of Power Sources*, 256, 369 – 382.

Boyd, S., Ghaoui, L.E., Feron, E., Balakrishnan, V., and Yakubovich, V.A. (1995). Linear matrix inequalities in system and control theory. *SIAM Review*, 37(3), 479–480.

Boyd, S.P., El Ghaoui, L., Feron, E., and Balakrishnan, V. (1994). *Linear matrix inequalities in system and control theory*, volume 15. SIAM.

Buller, S., Karden, E., Kok, D., and De Doncker, R.W. (2001). Modeling the dynamic behavior of supercapacitors using impedance spectroscopy. In *Proc. of the 36th IAS Annual Meeting of the Industry Applications Conference*, volume 4, 2500–2504. IEEE, Chicago, IL.

Burke, A. (2000). Ultracapacitors: Why, how, and where is the technology. *Journal of power sources*, 91(1), 37–50.

d'Entremont, A. and Pilon, L. (2014). First-principles thermal modeling of electric double layer capacitors under constant-current cycling. *Journal of Power Sources*, 246, 887–898.

Dey, S., Mohon, S., and Onori, S. (2016). Model-based sensor fault diagnostics of double-layer capacitors. In *Proc. of the American Control Conference*, 1512–1517. Boston, USA.

Drummond, R., Howey, D.A., and Duncan, S.R. (2015). Low-order mathematical modelling of electric double layer supercapacitors using spectral methods. *Journal of Power Sources*, 277, 317–328.

Drummond, R., Howey, D.A., and Duncan, S.R. (2016a). Parameter estimation of an electrochemical supercapacitor model. In *Proc. of the European Control Conference (ECC)*, 1–6. Aarlberg, Denamrk.

Drummond, R., Zhao, S., and Duncan, S. (2016b). Design tools for electrochemical supercapacitors using local absolute stability theory. *Under review at IEEE Transactions on Control Systems Tehcnology*.

Drummond, R., Zhao, S., Howey, D., and Duncan, S. (2017). Circuit synthesis of electrochemical supercapacitor models. *Journal of Energy Storage*, 10, 48 – 55.

Guillemin, E.A. (1977). *Synthesis of passive networks: Theory and methods appropriate to the realization and approximation problems*. RE Krieger Pub. Co., Malabar, Florida.

Khalil, H. (2002). *Nonlinear Systems*, volume 3. Prentice hall Upper Saddle River.

Lu, M., Beguin, F., and Frackowiak, E. (2013). *Supercapacitors: Materials, Systems and Applications*. John Wiley & Sons, Weinheim, Germany.

Rafik, F., Gualous, H., Gallay, R., Crausaz, A., and Berthon, A. (2007). Frequency, thermal and voltage supercapacitor characterization and modeling. *Journal of Power Sources*, 165(2), 928–934.

Robinson, D.B. (2010). Optimization of power and energy densities in supercapacitors. *Journal of Power Sources*, 195(11), 3748–3756.

Romero-Becerril, A. and Alvarez-Icaza, L. (2010). Reduced order dynamical model for supercapacitors. In *Proc. 7th IEEE International Conference on Electrical Engineering Computing Science and Automatic Control*, 71–76. Tuxtla Gutierrez, Mexico.

Sheberla, D., Bachman, J.C., Elias, J.S., Sun, C.J., Shao-Horn, Y., and Dincă, M. (2016). Conductive MOF electrodes for stable supercapacitors with high areal capacitance. *Accepted for publication in Nature Materials on 31st August 2016*.

Srinivasan, V. and Weidner, J.W. (1999). Mathematical modeling of electrochemical capacitors. *Journal of the Electrochemical Society*, 146(5), 1650–1658.

Valmorbida, G., Drummond, R., and Duncan, S.R. (2016). Positivity conditions of Lyapunov functions for systems with slope restricted nonlinearities. In *Proc. of the American Control Conference*, 258–263. Boston, USA.

Verbrugge, M.W. and Liu, P. (2005). Microstructural analysis and mathematical modeling of electric double-layer supercapacitors. *Journal of the Electrochemical Society*, 152(5), D79–D87.

von Srbik, M.T., Marinescu, M., Martinez-Botas, R.F., and Offer, G.J. (2016). A physically meaningful equivalent circuit network model of a lithium-ion battery accounting for local electrochemical and thermal behaviour, variable double layer capacitance and degradation. *Journal of Power Sources*, 325, 171–184.

Xia, M., Antsaklis, P.J., Gupta, V., and Zhu, F. (2012). Passivity and dissipativity analysis of a system and its approximation. *ISIS Technical Report ISIS-2012-007*.

Zhang, L., Wang, Z., Hu, X., Sun, F., and Dorrell, D.G. (2015). A comparative study of equivalent circuit models of ultracapacitors for electric vehicles. *Journal of Power Sources*, 274, 899–906.